EXPERIMENT AND NUMERICAL ANALYSIS OF MAGNETIC DIPOLE INTERACTIONS AMONG FEEBLE MAGNETIC SUBSTANCES UNDER HIGH MAGNETIC FIELD

T. Ando[1]*, N. Hirota*[1]*, A. Satoh*[2]*, E. Beaugnon*[3]

[1] *Tsukuba Magnet Laboratory, National Institute for Materials Science, Sakura 3-13, 305-0003 Tsukuba, Japan (ANDO.Tsutomu@nims.go.jp)*
[2] *Department of Machine Intelligence and Systems Engineering, Akita Prefectual University, Japan*
[3] *Centre National de la Recherche Scientifique, CRETA, France*

Introduction. In recent years, a high magnetic field with the strength of several Tesla can be generated using superconducting magnets, so that significant effects on para- and diamagnetic substances, namely, feeble magnetic substances caused by such magnetic field are recognized [1]–[5]. These effects are mainly based on interactions between fields and feeble magnetic substances. In a series of studies using high magnetic field, however, Takayama *et al.* [6] observed interactions acting among magnetic dipoles induced in feeble substances and triangle-lattice alignments with some spacing formed by them in the air-liquid surface without friction. Since almost all the materials on the earth are feeble magnetic substances, it is suggested from their results that a high magnetic field enables us to arrange substances and to control the internal structure of a substance.

In the present study, we investigate the two-dimensional triangle-lattice alignments with some spacing by means of experiment and numerical simulation. First, we carried out experiments, in which the gold particles were dispersed in a closed vessel filled with a medium. Next, we developed a simulation model based on the molecular dynamics (MD) method and investigated the motion of particles in aqueous solution. The results between experiment and numerical simulation are quantitatively compared.

1. Experiment.

1.1. Experimental conditions. The experimental setup is shown in Fig. 1 and also the physical conditions in the experiment and numerical simulation are indicated in Table 1. The triangle-lattice structure of gold particles on the air-liquid interface with a petri dish was observed by Takayama *et al.* [6]. When the air-liquid interface exists, it is difficult to evaluate accurately the magnetic dipole moment because the particle is levitated and its head is exposed to the air. In addition, the air-liquid interface also exerts the surface tension on particles. Therefore, in order to eliminate these unknown factors, we used the closed vessel and observed the formed structure in it, as shown in Fig. 1.

1.2. Experimental results. The experiment for the number of particle, $N = 100$, has been performed. Fig. 2a shows a typical configuration of $N = 100$. On this photo, it is confirmed that gold particles with a 1 mm diameter form the triangle-lattice alignments with some spacing and that the particle-particle distance in the center is relatively narrow, and this distance increases gradually with apart from the center.

2. Numerical simulation.

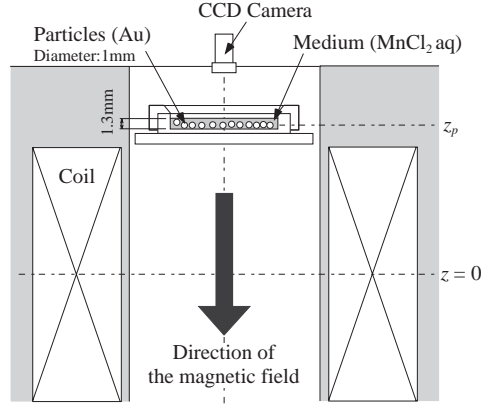*2.1. Numerical model for simulation.* The assumptions used in the numerical simulation are mainly as follows.

T. Ando, N. Hirota, A. Satoh, E. Beaugnon

Fig. 1. Experimental setup.

(i) The inertial force of the aqueous solution can be ignored because the Reynolds number of particle is very small.

(ii) The change of magnetic field in a particle can be ignored and its value can be regarded as a magnetic field at the particle center because particle is very small.

(iii) Particles are sufficiently diluted in the medium, so that hydrodynamic interactions among particles are negligible.

We have used the notation $U_i^{(H)}$ for the total potential energy of gravitation and the interaction between particle i and applied magnetic field $\mathbf{H}$ and also $U_{ij}^{(m)}$ for the magnetic dipole interaction energy among particles i and j. Then, the expressions for these quantities are written as

$$U_i^{(H)} = \frac{\pi d_p{}^3}{6} \left[-\frac{1}{2\mu_0}(\chi_p - \chi_f)\mathbf{B}_i{}^2 + (\rho_p - \rho_f)g z_i \right] , \qquad (1)$$

$$U_{ij}^{(m)} = \frac{\mu_f}{4\pi r_{ij}{}^3} \left[(\mathbf{m}_i \cdot \mathbf{m}_j) - \frac{3}{r_{ij}}(\mathbf{m}_i \cdot \mathbf{r}_{ij})(\mathbf{m}_j \cdot \mathbf{r}_{ij}) \right] , \qquad (2)$$

where $\mathbf{r}_{ij} = \mathbf{r}_i - \mathbf{r}_j$, $r_{ij} = \mid \mathbf{r}_{ij} \mid$, $r_i = \mid \mathbf{r}_i \mid$ and z_i is the position of particle i for r- and z-directions, respectively, and g is the acceleration of gravity. Since χ_p and $\chi_f \ll 1$, we regard $\mathbf{H} \simeq (1/\mu_0)\mathbf{B}$. The effective dipole moment $\mathbf{m}_i$ in

Table 1. Physical conditions of experiment and numerical simulation.

	Nomenclature		Value
Particle (Au)	Diameter	d_p [mm]	1.0
	Volume magnetic susceptibility	χ_p [-(SI)]	-3.45 $\times 10^{-5}$
	Density	ρ_p [kg/m^3]	1.93 $\times 10^4$
Medium (MnCl$_2$ aq)	Concentration	C [wt%]	40
	Volume magnetic susceptibility	χ_f [-(SI)]	7.99 $\times 10^{-4}$
	Density	ρ_f [kg/m^3]	1.39 $\times 10^3$
	Viscosity	η_f [mPa·s]	8.32±1
Imposed magnetic field	Position of particle	z_p [mm]	148±1
	Direction	—	z
	Amplitude at z_p	B_0 [T]	(4.9)

Eq. (2) denotes the induced magnetic dipole moment of diamagnetic particle i in the medium, and it is represented by the following equation [7]:

$$\mathbf{m}_i = \frac{\pi d_p{}^3}{2} \frac{\mu_p - \mu_f}{\mu_p + 2\mu_f} \mathbf{H}_i .$$ (3)

At $z = 148$ mm, the ratio of B_r/B_z is very small. Therefore, we ignore the r-component of $\mathbf{H}$ and carry out the two-dimensional simulation, that is, all magnetic dipole moments turn to the z-direction.

2.2. Equations of motion. The motion of an arbitrary particle i in the model system is governed by the following equation, which is expressed in a non-dimensional form:

$$\frac{\mathrm{d}\mathbf{v}^*{}_i}{\mathrm{d}t} = \sum_{i \neq j}^{N} \mathbf{F}_{ij}^{(m)^*} + \mathbf{F}_i^{(H)^*} - \mathbf{F}_i^{(v)^*} .$$ (4)

Each force in the above equation denotes

$$\mathbf{F}_{ij}^{(m)^*} = R_{ij}^{(m)} \frac{1}{r_{ij}^{*4}} \mathbf{t}_{ij} , \quad \mathbf{F}_i^{(H)^*} = R_i^{(H)} \mathbf{t}_i , \quad \mathbf{F}_i^{(v)^*} = R^{(v)} \mathbf{v}_i^* .$$ (5)

where $\mathbf{F}_{ij}^{(m)^*}$, $\mathbf{F}_i^{(H)^*}$ and $\mathbf{F}_i^{(v)^*}$ are the magnetic interaction force between particles i and j, the magnetic force that the applied magnetic field exerts on particle i and the viscous drag by the medium, respectively. The unit vectors $\mathbf{t}_{ij}$ and $\mathbf{t}_i$ are given by $\mathbf{t}_{ij} = \mathbf{r}_{ij}/r_{ij}$ and $\mathbf{t}_i = \mathbf{r}_i/r_i$. $\mathbf{v}_i^*$ is the velocity of particle i. The dimensionless parameters $R_{ij}^{(m)}$, $R_i^{(H)}$ and $R^{(v)}$ are normalized by the representative force $F_{r0}^{(m)}$. The representative length and time are d_p and $T = (md_p/F_{r0}^{(m)})^{1/2}$, respectively, where m is the mass of a particle.

3. Results and discussions. Here, we discuss the final configuration formed by particles at a steady state.

3.1. Final particle position at a steady state. The final configurations for the particle number $N = 100$ are shown in Fig. 2b. The maximum number of time steps is 4.5×10^5. The result of the final configurations show that the particle density is relatively high in the central part and becomes relatively lower in the outer part, as in the experiments.

3.2. Three-body distribution function. In order to analyze quantitatively the final configuration of particles in the numerical simulation, we defined the three-body distribution function $f_3(r,\theta)$. The three-body distribution function $f_3(r,\theta)$ represents the probability density function with respect to the two variables of r-θ. That is, $f_3(r,\theta)\Delta r \Delta \theta$ means the probability of $(r - \Delta r/2) \sim (r + \Delta r/2)$

(a) Experiment

(b) Numerical analysis

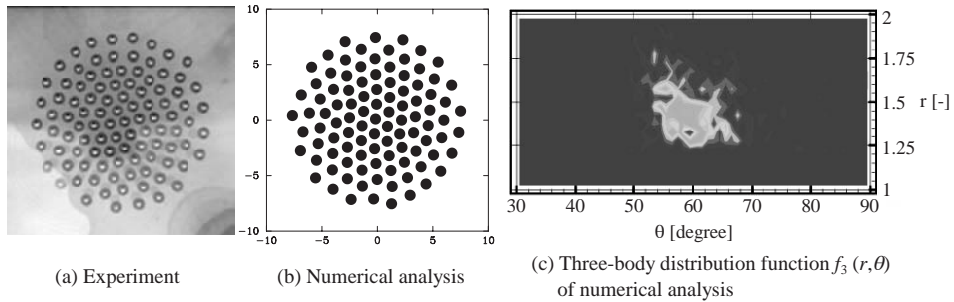(c) Three-body distribution function $f_3(r,\theta)$ of numerical analysis

Fig. 2. Results of experiment and numerical analysis for $N = 100$.
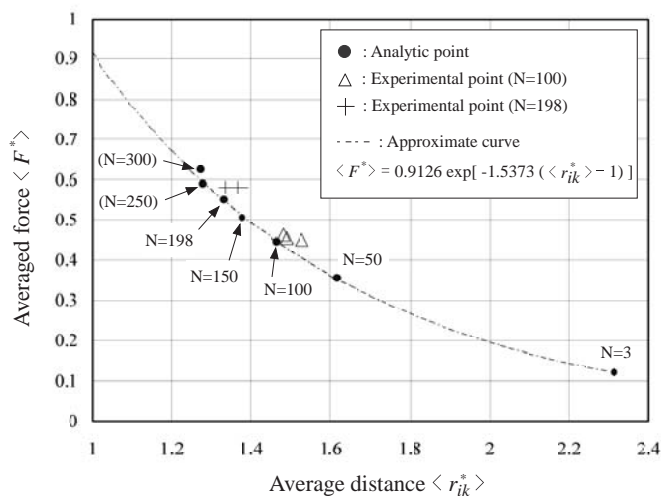
Fig. 3. The relation between the distance among particles and the interaction force at a steady state.

and $(\theta - \Delta\theta/2) \sim (\theta + \Delta\theta/2)$. The result of the three-body distribution function $f_3(r, \theta)$ for $N = 100$ is shown in Fig. 2c. $f_3(r, \theta)$ is calculated by taking account of all particles. It is seen that both results have a peak near $60°$ at a certain r range and the gathering particles form the triangle-lattice alignments.

3.3. Particle-particle distance and interaction force. We examined the relation between an average distance among particles $\langle r_{ik}^* \rangle$ and an averaged force per particle $\langle \mathbf{F}^* \rangle = \mid \mathbf{F}^{(H)^*} \mid_{Ave.} + \mid \mathbf{F}^{(m)^*} \mid_{Ave.}$, and plotted these data in Fig. 3 for seven analytic points, $N = 3, 50, 100, 150, 198, 250$ and 300. The average distance is obtained from $\langle r_{ik}^* \rangle = \sum_r^{all} \sum_\theta^{all} [r_{ik}^*]_{r,\theta} \times [f_3(r, \theta)]_{r,\theta}$. Here the range of distance of $f_3(r, \theta)$ was adopted in $1 \leq r^* \leq 1.9$ for $N = 250$ and 300 so that we can pick up the nearest particles around the particle i.

Besides, using an image analysis software, we added the points obtained from the experimental results to Fig. 3. These averaged forces $\langle \mathbf{F}^* \rangle$ are derived by using the numerical model. The experimental points for $N = 100$ significantly agree with the analytic point. And also, the experimental points for $N = 198$ are fairly equal to that of simulation.

REFERENCES

1. E. Beaugnon, R. Tournier. Levitation of organic materials. *Nature*, vol. 349 (1991), pp. 470.

2. S. Ueno, M. Iwasaka. Properties of diamagnetic fluid in high gradient magnetic fields. *J. Appl. Phys.*, vol. 75 (1994), no. 10, pp. 7177–7179.

3. M.A. Weilert, D.L. Whitaker, H.J. Maris, G.M. Seidel. Magnetic levitation and noncoalescence of liquid helium. *Phys. Rev. Lett.*, vol. 77 (1996), no. 23, pp. 4840–4843.

4. M.V. Berry, A.K. Geim. Of flying frogs and levitations. *Eur. J. Phys.*, vol. 18 (1997), pp. 307–313.

5. Y. Ikezoe, N. Hirota, J. Nakagawa, K. Kitazawa. Making water levitate. *Nature*, vol. 393 (1998), pp. 749–750.

6. T. Takayama, Y. Ikezoe, H. Uetake, N. Hirota, K. Kitazawa. Interactions among magnetic dipoles induced in feeble magnetic substances under high magnetic fields. *Physica B.*, vol. 346–347 (2004), pp. 272–276.

7. T.B. Jones. *Electromechanics of Particles.* (Cambridge University Press, New York, 1995).